Preprint version of the article:
S. R. Nekoo, J. A. Acosta, G. Heredia, and A. Ollero, "A benchmark mechatronics platform to assess the inspection around pipes with variable pitch quadrotor for industrial sites," Mechatronics (79): 2021, 102641, 1-9.
DOI: https://doi.org/10.1016/j.mechatronics.2021.102641

A benchmark mechatronics platform to assess the inspection around pipes with variable pitch quadrotor for industrial sites

Saeed Rafee Nekoo, José Ángel Acosta, Guillermo Heredia and Anibal Ollero
GRVC Robotics Lab., Departamento de Ingeniería de Sistemas y Automática
Escuela Técnica Superior de Ingeniería, Universidad de Sevilla, Seville, Spain
saerafee@yahoo.com, {jaar, guiller, aollero}@us.es

Abstract

This paper investigates the inspection-of-pipe topic in a new framework, by rotation around a pipe, peculiar to industrial sites and refineries. The evolution of the ultimate system requires prototype design and preliminary tests. A new benchmark has been designed and built to mimic the rotation around a pipe, with the main purpose of assessing the different types of rotors and control systems. The benchmark control system presents a mechatronics package including mechanical design and machining, electronics and motor drive, motor-blade installation, computer programming, and control implementation. The benchmark is also modular, working with two modes of one- and two-degree-of-freedom (DoF), easily interchangeable. To cover a full rotation, conventional fixed-pitch drones fail to provide negative thrusts; nonetheless, variable-pitch (VP) rotor quadcopters can produce that in both directions. A closed-loop nonlinear optimal controller is chosen for real-time communication, so-called, "the state-dependent Riccati equation (SDRE)" approach. Optimal control policies are challenging for experimentation though it has been successfully done in this report. The advantage of the VP is also illustrated in a rotation plus radial motion in comparison with fixed-pitch rotors while a wind gust disturbs the inspection task. The proposed VP system compensated the disturbance while the fixed-pitch was pushed away by the wind gust. The solution methods to the SDRE were mixed, a closed-form exact solution for the one-DoF system, and a numerical one for the two-DoF. Solving the Riccati online in each time step is a critical issue that was effectively solved by the implementation approach, through online communication with MATLAB software. Both simulations and experiments have been performed along with a discussion to prove the application of VP systems in rotary-motion pipe inspection.

Keywords*:* SDRE, variable-pitch, mechatronics system, inspection, quadrotor, optimal control.

Preprint version of the article:
S. R. Nekoo, J. A. Acosta, G. Heredia, and A. Ollero, "A benchmark mechatronics platform to assess the inspection around pipes with variable pitch quadrotor for industrial sites," Mechatronics (79): 2021, 102641, 1-9.
DOI: https://doi.org/10.1016/j.mechatronics.2021.102641

1. Introduction

Aerial robots are becoming more and more popular in recent years as their wide variety of applications grows day by day. These applications range from cargo transportation [1], infrastructure inspection [2], and cinematography [3] to search and rescue in post-disaster situations [4]. Special attention is being paid by the industry to the inspection and maintenance with drones [5] in oil and gas plants, wind turbines [6], bridges [7], or power lines [8]. In particular, oil and gas industrial plants and refineries usually have thousands of kilometers of pipes that are exposed to corrosion and have to be periodically inspected, measuring pipe wall thickness with ultrasonic sensors to detect incipient corrosion and prevent spills. Besides, several measurements have to be done in each pipe section along the whole pipe diameter. A significant part of the pipes are located in difficult-to-access areas, and a logical approach is using robotic inspection systems, as crawlers and i.e. multirotor drones [9, 10].

The HYFLIERS (HYbrid FLying-rollIng with-snakE-aRm robot for contact inSpection) project was initiated to investigate pipe-inspection in refineries and industrial sites in the framework of a research and innovation action of the EU H2020 program [11]. One of the solutions that is being developed in the project is a hybrid robot that can fly to the pipe, land, and move along it to reach different inspection points, using a small manipulator arm with the ultrasonic sensor to reach the different measurement points around the pipe diameter [12, 13].

Another approach that is being considered is that the whole robot moves around the pipe, covering a full rotation to measure the wall thickness, avoiding the additional weight of the arm. The conventional multirotor design uses fixed-pitch propellers mainly due to their simpler mechanisms and easier control when compared with variable-pitch (VP) propellers. In the case of operation on the pipe with some grip mechanism, like magnets, the fixed-pitch solution seems to be suitable because its control, while operating on the pipe, is reduced to switch the magnet and this is the case of the hybrid robotic systems. On the other hand, when the design does not have a grip mechanism the variable-pitch solution becomes more advantageous because its ability to generate negative thrust (unlike the fixed-pitch one) becomes necessary to keep the multirotor position under circumstances such as inaccurate landing position due to wind disturbances or clearance for the gripper.

The variable-pitch propellers date back to airplanes, helicopters, and marine vessels [14, 15]; though the most relevant studies were among the literature on helicopters. A VP quadcopter uses the same idea but for four rotors. The symmetrical assembly and lightweight system make

Preprint version of the article:
S. R. Nekoo, J. A. Acosta, G. Heredia, and A. Ollero, "A benchmark mechatronics platform to assess the inspection around pipes with variable pitch quadrotor for industrial sites," Mechatronics (79): 2021, 102641, 1-9.
DOI: https://doi.org/10.1016/j.mechatronics.2021.102641

the design easier than a helicopter, although it also includes an additional actuator and the linking mechanism that, in practice, is usually mechanically weak. That is why the role of VP quadrotors are not highlighted recently in the research nevertheless helicopters with VP rotor design and swashplate work perfectly well [16].

The application of variable-pitch quadrotors was reported by Langkamp and Crowther 2010 [17], and Cutler et al. [18]. Endurance of the VP system in a windy environment was reported as the key advantage in comparison with a fixed-pitch quadcopter; a moderate collective pitch increased the endurance of the flying system [17]. Other superiorities could be listed as an increased change in thrust rate, decreased saturation inputs, and efficiently changing thrust direction [19]. Performance comparisons of VP and fixed-pitch quadrotors were made in terms of climb rate and flight endurance [20]. The ability to provide a negative thrust for the drone is one of the most important advantages of the VP systems. A particular example to highlight this point is the flip maneuver by a drone. The VP drones are capable of flip maneuver [21, 22]; and this motion also embraces the singularity problem of conventional systems (systems considering hovering condition for flights). In this current work, the motion somehow resembles a flip but is constrained to a circular motion. The negative thrust similarly provides the possibility of the controlled flip.

In this work, a benchmark is proposed to check the application of the variable-pitch rotors quadcopters for inspection of pipes by rotation. The flying system possesses VP rotors and a gripper to clamp around a pipe. After clamping, the operation could be mimicked by the proposed benchmark. The design includes working in two modes of one- and two DoFs: one-DoF considers pure rotation and two-DoF design include a small clearance in radial motion. The proposed system is a multidisciplinary mechatronics design covering: mechanical, electrical, aerospace, and control engineering. The two-DoF system could be viewed as a double pendulum. Double pendulums could be under-actuated systems [23], or redundantly actuated [24]. Fradkov et al. presented a multi-pendulum benchmark to assess the implementation of different algorithms and estimation methods [25]. The role of the proposed benchmark in this current design is also an assessment of the total operation (rotation around a pipe) and control implementation.

An optimal control policy has been selected as the base of the control design to ensure a trade-off between energy and precision and also benefit from optimality and robustness. A good nominee with the mentioned characteristics is the state-dependent Riccati equation [26]. A

Preprint version of the article:
S. R. Nekoo, J. A. Acosta, G. Heredia, and A. Ollero, "A benchmark mechatronics platform to assess the inspection around pipes with variable pitch quadrotor for industrial sites," Mechatronics (79): 2021, 102641, 1-9.
DOI: https://doi.org/10.1016/j.mechatronics.2021.102641

quadratic cost function enables the trade-off by tuning the weighting matrices. The controller has been widely used in different areas such as aerospace [27], robotics [28], missile [29], permanent magnet synchronous motors [30], pendulums [31], atomic force microscopy [32], etc. The application of the SDRE in quadrotor control was reported for the first time in 2006 [33]. Then it expanded for different drones [34], unmanned small helicopters [35]; and employed in VP rotor quadcopter control [21, 22, 36]. The relation between the input force and moments of a VP unmanned aerial vehicle (UAV) and blade angles of the rotors is nonlinear, which requires thrust allocation. Bhargavapuri et al. presented a stable first-order dynamic for thrust allocation of the system then transferred them into PWM to actuate the blades [21]. Optimal thrust allocation using the SDRE controller was addressed for this topic in four different methods [22]. In this current research, the theoretical design of the SDRE is implemented on a novel experimental platform (with VP rotor design) for validating the rotary motion around a pipe for inspection, as close as possible to reality.

The main contributions of this work are: designing and manufacturing a novel experimental setup for one- and two-DoF motion control of a system to emulate the inspection of pipes task with quadrotors flying around them, radial and rotary motion; the full assessment of both variable-pitch and fixed-pitch multirotors together with their control systems and the online implementation of the SDRE on VP rotor systems for the first time.

Section 2 presents the dynamics of the system. Section 3 reports the SDRE. The implementation technique is presented in Section 4. Section 5 describes the platform. Results and concluding remarks are also expressed in Section 6 and 7.

2. Dynamics: System Modeling

The rotation around a pipe could be modeled in two modes: one degree-of-freedom and two-DoF. In the first case, the only engaged variable is $\theta(\mathrm{rad})$, representative of rotation around the center of the pipe, see Fig. 1. The second case is more challenging and represents a new structure by a variable-pitch quadrotor for modeling of a rotation around the pipe with additional motion in a radial direction, r (m). Both modeling methods are logical and operational, one-DoF with a rolling clamp and the second one with additional clearance in the radial direction. The ability to provide negative thrust by VP rotors are the key to both designs.

Preprint version of the article:
S. R. Nekoo, J. A. Acosta, G. Heredia, and A. Ollero, "A benchmark mechatronics platform to assess the inspection around pipes with variable pitch quadrotor for industrial sites," Mechatronics (79): 2021, 102641, 1-9.
DOI: https://doi.org/10.1016/j.mechatronics.2021.102641

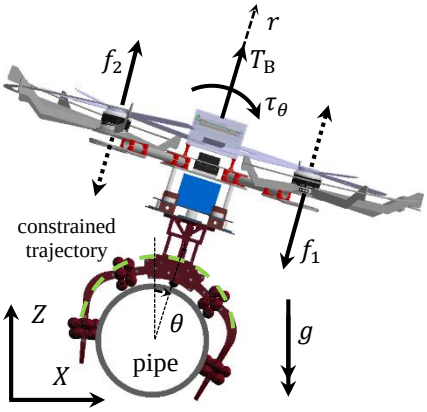

Fig. 1. The schematic presentation of a quadrotor, clamping around a pipe for rotation and inspection.

2-1. One-DoF modeling, pure rotation

This section presents the dynamics of a UAV, landed on a pipe and clamped around it. This case changes the equation of motion to a rotating object around a point. The clamps have wheels at their ends, hence the friction is negligible. The motion of the UAV is in the XZ plane, on a circular path. The model of the system after landing is similar to a rotating one-degree-of-freedom pendulum:

$$\left(mr_{\text{ctr}}^2 + I_{yy}\right)\ddot{\theta}(t) + mgr_{\text{ctr}} \sin\theta(t) = \tau_\theta(t), \quad \textbf{(1)}$$

where r_{ctr} (m) is the distance between the center of the pipe and CoM of the quadrotor, m (kg) is the weight of the setup, g (m/s^2) represents the gravity constant and $\tau_\theta(\text{N.m})$ is the input torque. We select the state vector as $\mathbf{x}(t) = \left[\theta(t), \dot{\theta}(t)\right]^T$ in which $\dot{\theta}$ (rad/s) presents the angular velocity of the system around the pipe. Considering the dynamics (1), the state-space representation of the VP in one-DoF mode is:

$$\dot{\mathbf{x}}(t) = \begin{bmatrix} \dot{\theta}(t) \\ \frac{\tau_\theta(t) - mgr_{\text{ctr}} \sin\theta(t)}{mr_{\text{ctr}}^2 + I_{yy}} \end{bmatrix}. \quad \textbf{(2)}$$

2-2. Two-DoF modeling, rotation, and translation

A radial motion is added to the rotation of the quadrotor concerning Subsection II-A. The motion is in the direction of a line between the center of the pipe and the CoM of the quadrotor. The motion range is also small, limited by the clearance of the clamp around the pipe. The two-DoF motion of the system is in XZ plane, Fig. 1. Selecting the generalized coordinates of the system as $\mathbf{q}(t) = \{r(t), \theta(t)\}$ (m, rad), the equation of motion finds the form

Preprint version of the article:
S. R. Nekoo, J. A. Acosta, G. Heredia, and A. Ollero, "A benchmark mechatronics platform to assess the inspection around pipes with variable pitch quadrotor for industrial sites," Mechatronics (79): 2021, 102641, 1-9.
DOI: https://doi.org/10.1016/j.mechatronics.2021.102641

$$\mathbf{M}\big(\mathbf{q}(t)\big)\ddot{\mathbf{q}}(t) + \mathbf{c}\big(\dot{\mathbf{q}}(t), \mathbf{q}(t)\big) + \mathbf{g}\big(\mathbf{q}(t)\big) = \mathbf{u}(t), \tag{3}$$

where inertia matrix is $\mathbf{M}\big(\mathbf{q}(t)\big)$, Coriolis and centrifugal vector is $\mathbf{c}\big(\dot{\mathbf{q}}(t), \mathbf{q}(t)\big)$, gravity vector is $\mathbf{g}\big(\mathbf{q}(t)\big)$ and input vector is $\mathbf{u}(t)$:

$$\mathbf{M}\big(\mathbf{q}(t)\big) = \begin{bmatrix} m & 0 \\ 0 & mr^2(t) + I_{yy} \end{bmatrix}, \mathbf{c}\big(\dot{\mathbf{q}}(t), \mathbf{q}(t)\big) = \begin{bmatrix} -mr(t)\dot{\theta}^2(t) \\ 2mr(t)\dot{r}(t)\dot{\theta}(t) \end{bmatrix},$$

$$\mathbf{g}\big(\mathbf{q}(t)\big) = \begin{bmatrix} mg\cos\theta(t) \\ -r(t)g\sin\theta(t) \end{bmatrix}, \mathbf{u}(t) = \begin{bmatrix} T_{\mathrm{B}}(t) \\ \tau_\theta(t) \end{bmatrix}.$$

The reference coordinate is set in the center of the pipe. The state-vector of the system is chosen $\mathbf{x}(t) = \big[r(t), \theta(t), \dot{r}(t), \dot{\theta}(t)\big]^T$, and it transforms the equation of motion (3) to the state-space representation of the quadrotor

$$\dot{\mathbf{x}}(t) = \begin{bmatrix} \dot{r}(t) \\ \dot{\theta}(t) \\ \mathbf{M}^{-1}\big(\mathbf{x}(t)\big)\big[\mathbf{u}(t) - \mathbf{c}\big(\mathbf{x}(t)\big) - \mathbf{g}\big(\mathbf{x}(t)\big)\big] \end{bmatrix}. \tag{4}$$

3. Controller Design: State-dependent Riccati Equation

The state-dependent Riccati equation is a controller with nonlinear and optimal themes, applicable for the systems in the form of

$$\dot{\mathbf{x}}(t) = \mathbf{f}\big(\mathbf{x}(t)\big) + \mathbf{g}\big(\mathbf{x}(t), \mathbf{u}(t)\big). \tag{5}$$

With the help of an important transformation so-called, state-dependent coefficient (SDC) parameterization, the new representation is found [37]:

$$\begin{aligned} \mathbf{f}\big(\mathbf{x}(t)\big) &= \mathbf{A}\big(\mathbf{x}(t)\big)\mathbf{x}(t), \\ \mathbf{g}\big(\mathbf{x}(t), \mathbf{u}(t)\big) &= \mathbf{B}\big(\mathbf{x}(t)\big)\mathbf{u}(t). \end{aligned} \tag{6}$$

The $\mathbf{g}\big(\mathbf{x}(t), \mathbf{u}(t)\big)$ and $\mathbf{f}\big(\mathbf{x}(t)\big)$ vectors, in (5), are piecewise continuous and smooth functions that satisfy the Lipschitz condition. $\mathbf{x}(t) \in \mathbb{R}^n$ is a state-vector and $\mathbf{u}(t) \in \mathbb{R}^m$ is an input vector, and the SDC matrices $\mathbf{A}\big(\mathbf{x}(t)\big): \mathbb{R}^n \to \mathbb{R}^{n\times n}$ and $\mathbf{B}\big(\mathbf{x}(t)\big): \mathbb{R}^n \to \mathbb{R}^{n\times m}$, in (6), are held. Optimal control policy applies by the cost function integral

$$J = \frac{1}{2}\int_0^\infty \big\{\mathbf{x}^T(t)\mathbf{Q}\big(\mathbf{x}(t)\big)\mathbf{x}(t) + \mathbf{u}^T(t)\mathbf{R}\big(\mathbf{x}(t)\big)\mathbf{u}(t)\big\}\mathrm{d}t,$$

where $\mathbf{Q}\big(\mathbf{x}(t)\big): \mathbb{R}^n \to \mathbb{R}^{n\times n}$ is a weighting matrix for states and $\mathbf{R}\big(\mathbf{x}(t)\big): \mathbb{R}^n \to \mathbb{R}^{m\times m}$ is one for inputs; both of them symmetric and positive. $\mathbf{Q}\big(\mathbf{x}(t)\big)$ could be semi-definite though $\mathbf{R}\big(\mathbf{x}(t)\big)$ must be definite.

Preprint version of the article:
S. R. Nekoo, J. A. Acosta, G. Heredia, and A. Ollero, "A benchmark mechatronics platform to assess the inspection around pipes with variable pitch quadrotor for industrial sites," Mechatronics (79): 2021, 102641, 1-9.
DOI: https://doi.org/10.1016/j.mechatronics.2021.102641

Controllability. $\{\mathbf{A}(\mathbf{x}(t)), \mathbf{B}(\mathbf{x}(t))\}$ is a completely controllable parameterization of the system (5). This implies that the controllability matrix must be full rank [38]:

$$\mathbf{M}_{\mathrm{c}}(\mathbf{x}(t)) = [\, \mathbf{B}(\mathbf{x}(t)), \mathbf{A}(\mathbf{x}(t))\mathbf{B}(\mathbf{x}(t)), \dots, \mathbf{A}^{n-1}(\mathbf{x}(t))\mathbf{B}(\mathbf{x}(t)) \,].$$

The controllability matrix should be full rank at the equilibrium point $\mathbf{M}_{\mathrm{c}}(\mathbf{0})$, and also in $(0, t_{\mathrm{f}}]$. checking $\mathbf{M}_{\mathrm{c}}(\mathbf{0})$ could be done off-line, however, a simulation is needed to realize the state of $\mathbf{M}_{\mathrm{c}}(\mathbf{x}(t))$ in $(0, t_{\mathrm{f}}]$.

Observability. $\{\mathbf{A}(\mathbf{x}(t)), \mathbf{Q}^{1/2}(\mathbf{x}(t))\}$ is a completely observable parameterization of the system (5); which expresses that the observability matrix must be full rank [38]:

$$\mathbf{M}_{\mathrm{o}}(\mathbf{x}(t)) = \begin{bmatrix} \mathbf{Q}^{1/2}(\mathbf{x}(t)) \\ \mathbf{Q}^{1/2}(\mathbf{x}(t))\mathbf{A}(\mathbf{x}(t)) \\ \vdots \\ \mathbf{Q}^{1/2}(\mathbf{x}(t))\mathbf{A}^{n-1}(\mathbf{x}(t)) \end{bmatrix}.$$

The observability matrix should be full rank at the equilibrium point $\mathbf{M}_{\mathrm{o}}(\mathbf{0})$, and also in $(0, t_{\mathrm{f}}]$.

The control law of the state-dependent Riccati equation is found by applying the optimality condition on the Hamiltonian:

$$\mathbf{u}(t) = -\mathbf{R}^{-1}(\mathbf{x}(t))\mathbf{B}^{T}(\mathbf{x}(t))\mathbf{K}(\mathbf{x}(t))\mathbf{x}(t), \tag{7}$$

where $\mathbf{K}(\mathbf{x}(t))$: $\mathbb{R}^n \to \mathbb{R}^{n\times n}$ is the symmetric positive definite solution to the SDRE:

$$\mathbf{A}^{T}(\mathbf{x})\mathbf{K}(\mathbf{x}) + \mathbf{K}(\mathbf{x})\mathbf{A}(\mathbf{x}) - \mathbf{K}(\mathbf{x})\mathbf{B}(\mathbf{x})\mathbf{R}^{-1}(\mathbf{x})\mathbf{B}^{T}(\mathbf{x})\mathbf{K}(\mathbf{x}) + \mathbf{Q}(\mathbf{x}) = \mathbf{0}. \tag{8}$$

4. Implementation

4-1. One-DoF model, an exact solution to SDRE

The SDC matrices of the system (2) are

$$\mathbf{A}(\mathbf{x}(t)) = \begin{bmatrix} 0 & 1 \\ -\dfrac{c_1 \sin x_1(t)}{x_1(t)} & 0 \end{bmatrix}, \mathbf{B} = \begin{bmatrix} 0 \\ c_2 \end{bmatrix}, \tag{9}$$

in which $c_1 = \frac{mgr_{\mathrm{ctr}}}{mr_{\mathrm{ctr}}^2 + I_{yy}}$ and $c_2 = \frac{1}{mr_{\mathrm{ctr}}^2 + I_{yy}}$. A more proper form for $\mathbf{A}(\mathbf{x}(t))$ in (9) is to avoid singularity at equilibrium point using Taylor series expansion

$$\mathbf{A}(\mathbf{x}(t)) = \begin{bmatrix} 0 & 1 \\ -c_1\left(1 - \dfrac{x_1^2(t)}{6} + \cdots\right) & 0 \end{bmatrix}. \tag{10}$$

We consider general weighting matrices

Preprint version of the article:
S. R. Nekoo, J. A. Acosta, G. Heredia, and A. Ollero, "A benchmark mechatronics platform to assess the inspection around pipes with variable pitch quadrotor for industrial sites," Mechatronics (79): 2021, 102641, 1-9.
DOI: https://doi.org/10.1016/j.mechatronics.2021.102641

$$R(\mathbf{x}(t)), \mathbf{Q}(\mathbf{x}(t)) = \begin{bmatrix} Q_{11}(\mathbf{x}(t)) & 0 \\ 0 & Q_{22}(\mathbf{x}(t)) \end{bmatrix}, \tag{11}$$

for the control design, and put all the matrices, Eqs. (9)-(11), into (8) which results in

$$Q_{11} - \frac{c_2^2 K_{12}^2}{R} - 2c_1 K_{12}\left(1 - \frac{x_1^2(t)}{6}\right) = 0, \tag{12}$$

$$K_{11} - \frac{c_2^2 K_{12} K_{22}}{R} - c_1 K_{22}\left(1 - \frac{x_1^2(t)}{6}\right) = 0, \tag{13}$$

$$2K_{12} + Q_{22} - \frac{c_2^2 K_{22}^2}{R} = 0. \tag{14}$$

The SDRE (8) generates 4 algebraic equations. Since that is a symmetric equation, 3 equations are necessary for a solution, (12)-(14). The control law (7) is

$$u(t) = -\frac{c_2}{R(\mathbf{x}(t))}\left(K_{12}(\mathbf{x}(t))x_1(t) + K_{22}(\mathbf{x}(t))x_2(t)\right), \tag{15}$$

Solving the sets of equations (12)-(14), resulted from the SDRE, provides the gains:

$$K_{12}(\mathbf{x}) = \frac{1}{6c_2^2}\left(c_1 R[x_1^2 - 6] + \sqrt{R(36c_2^2 Q_{11} + c_1^2 R[x_1^2 - 6]^2)}\right), \tag{16}$$

$$K_{22}(\mathbf{x}) = \frac{1}{\sqrt{3}c_2}\left(3RQ_{22} - \frac{6c_1R^2}{c_2^2} + \frac{c_1R^2x_1^2}{c_2^2} + \frac{R}{c_2^2}\sqrt{36c_2^2Q_{11}R + (6c_1R - c_1Rx_1^2)^2}\right)^{1/2}. \tag{17}$$

It is possible to solve the SDRE as an exact solution approach for the one-DoF model by substituting (16) and (17) into (15). The scalar control input $u(t)$ is mapped and scaled into the allowable range of servo actuators that changes the blade angles of VP rotors. There are two servo motors in the one-DoF model, so the mapped input with different signs actuates the servos symmetrically.

4-2. Two-DoF model

The SDC parameterization of equation (4) is

$$\mathbf{A}(\mathbf{x}(t)) = \begin{bmatrix} \mathbf{0}_{2\times2} & \mathbf{I}_{2\times2} \\ \mathbf{0}_{2\times2} & -\mathbf{M}^{-1}(\mathbf{x}(t))\mathbf{C}(\mathbf{x}(t)) \end{bmatrix},$$

$$\mathbf{B}(\mathbf{x}(t)) = \begin{bmatrix} \mathbf{0}_{2\times2} \\ \mathbf{M}^{-1}(\mathbf{x}(t)) \end{bmatrix},$$

Preprint version of the article:
S. R. Nekoo, J. A. Acosta, G. Heredia, and A. Ollero, "A benchmark mechatronics platform to assess the inspection around pipes with variable pitch quadrotor for industrial sites," Mechatronics (79): 2021, 102641, 1-9.
DOI: https://doi.org/10.1016/j.mechatronics.2021.102641

in which $\mathbf{C}(\mathbf{x}(t)) = \begin{bmatrix} 0 & -mr(t)\dot{\theta}(t) \\ 2mr(t)\dot{\theta}(t) & 0 \end{bmatrix}$. The gravity vector in the two-DoF model includes $\cos(\cdot)$ function and the Taylor series expansion of that presents a constant in the first term. So, it cannot be factored similar to $\sin(\cdot)$ in Eq. (10). A well-known method is to add gravity to control law [39]:

$$\mathbf{u}(t) = -\mathbf{R}^{-1}(\mathbf{x}(t))\mathbf{B}^{T}(\mathbf{x}(t))\mathbf{K}(\mathbf{x}(t))\mathbf{x}(t) + \mathbf{g}(\mathbf{x}(t)), \quad \textbf{(18)}$$

in which the gain $\mathbf{K}(\mathbf{x}(t))$ of the SDRE must be found by a numerical solution to (8). An increase in the dimension of the system and complexity of matrices prevent us from finding an exact solution to the SDRE, similar to the pure rotation model, in Section IV-A.

The control input provides a force, total thrust T_{B}, and a torque τ_θ against the rotary motion, Fig. 1. These inputs have a relation with thrust coefficients of VP rotors of the setup:

$$\begin{bmatrix} T_{\mathrm{B}}(t) \\ \tau_\theta(t) \end{bmatrix} = k \begin{bmatrix} 1 & 1 \\ -l & l \end{bmatrix} \begin{bmatrix} C_{\mathrm{T},1}(t) \\ C_{\mathrm{T},2}(t) \end{bmatrix}, \quad \textbf{(19)}$$

where l (m) is the perpendicular distance between CoM of the system and rotor shaft, $k = \rho\pi R^4 \omega_{\mathrm{ss}}^2$ in which ρ (kg/m^3) is the air density, R (m) is the radius of the rotor, ω_{ss} (rad/s) is the steady-state angular velocity of the rotor, and $C_{\mathrm{T},i}(t)$ is the thrust coefficient of i-th rotor. Then the thrust coefficient is transformed to blade angles, $\alpha_i(t)$ (rad), for actuating the system, subject to upper/lower ($\alpha_{\max}$ and $\alpha_{\min}$) bounds:

$$\begin{cases} if\ \alpha_i(t) > \alpha_{max}, & \alpha_i(t) = \alpha_{max} \\ if\ \alpha_{min} \le \alpha_i(t) \le \alpha_{max}, & \alpha_i(t). \\ if\ \alpha_i(t) < \alpha_{min}, & \alpha_i(t) = \alpha_{max} \end{cases}$$

5. Experimental Platform

A special experimental platform is needed to validate the proposed models in Section II, one- and two-DoF rotating systems. Rotating around a pipe in outdoor facilities is the ultimate goal of the HYFLIERS project. The primary step is made to check the performance of the VP rotors in a controlled environment in a similar situation that resembles the pipe inspection, as presented in the schematic in Fig. 1. The primary setup is presented in Fig. 2. It has the option of working in two modes: one- and two-degree-of-freedom. There is a pin at the center of the setup for holding the system in one-DoF mode. If one removes the pin, the system moves in a radial r direction as well. The operation of switching modes could be observed in Fig. 4.

Preprint version of the article:
S. R. Nekoo, J. A. Acosta, G. Heredia, and A. Ollero, “A benchmark mechatronics platform to assess the inspection around pipes with variable pitch quadrotor for industrial sites,” Mechatronics (79): 2021, 102641, 1-9.
DOI: https://doi.org/10.1016/j.mechatronics.2021.102641

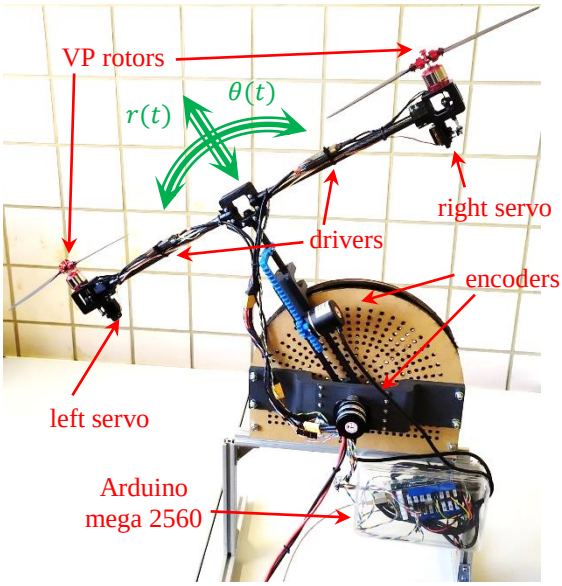

Fig. 2. The experimental platform of the partial rotation around a pipe.

(a) (b)

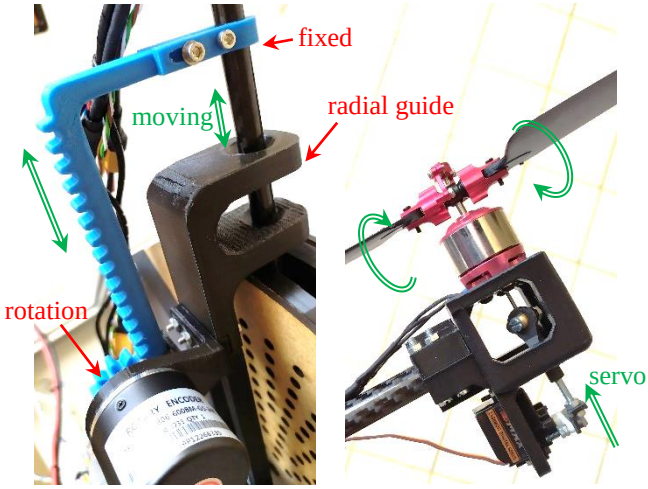

Fig. 3. (a) Detailed view of the rack and pinion mechanism for linear motion measurement; (b) detail view of the variable pitch mechanism.

Preprint version of the article:
S. R. Nekoo, J. A. Acosta, G. Heredia, and A. Ollero, "A benchmark mechatronics platform to assess the inspection around pipes with variable pitch quadrotor for industrial sites," Mechatronics (79): 2021, 102641, 1-9.
DOI: https://doi.org/10.1016/j.mechatronics.2021.102641

(a) (b)

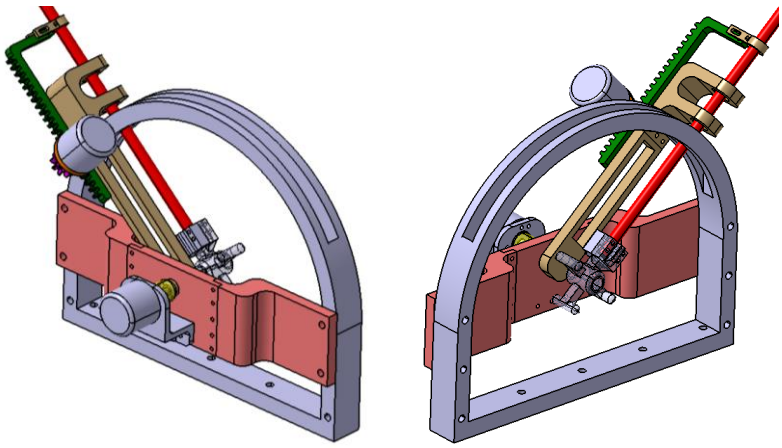

Fig. 4. Design and detailed views of the setup; (a) front view, (b) back view.

The setup consists of EVP-22 brushless DC (BLDC) motors with metallic variable-pitch mechanism (Fig. 3-a), DJI E305 420 LITE drivers with 20A allowable current and 17.4V allowable voltage, ES08MDII micro digital servos with 2kg.cm torque at 4.8V operating voltage. The measurement system employs optical rotary encoders LPD3806, 600 pulses per revolution with mechanical attachment to the system. The rotary motion, $\theta(t)$, measurement is directly made; however, the linear motion $r(t)$ needs a customized rack and pinion design for the transformation of the linear movement to the rotation, the blue 3D printed parts in the center of the image in Fig. 3-b. The digital board, responsible for communication with the computer, is Arduino Mega 2560. The specifications of the setup are presented in Table 1.

Table 1. The specifications of the setup.

Para.	value	unit	description
l	0.29	m	Dist. between CoM and rotor shaft
R	0.135	m	radius of propeller
I_{yy}	9.354×10^3	kg.m^2	moment of inertia
m	0.870	kg	total weight of the setup
k	3.32×10^{-6}	$\frac{\text{N.s}^2}{\text{rad}^2}$	lift constant - thrust factor

The main coding for experimentation is done in MATLAB software with online communication with the setup. The methodology is similar to the digital implementation of a nonlinear optimal control with time-varying sampling time [40]. Arduino package is used that provides several functions such as reading encoders, writing servo commands, and PWM signals in the MATLAB script environment. This allows us to use several other useful commands and complex mathematical operations in the same environment.

Preprint version of the article:
S. R. Nekoo, J. A. Acosta, G. Heredia, and A. Ollero, "A benchmark mechatronics platform to assess the inspection around pipes with variable pitch quadrotor for industrial sites," Mechatronics (79): 2021, 102641, 1-9.
DOI: https://doi.org/10.1016/j.mechatronics.2021.102641

The structure of the program consists of: loading Arduino package, assigning the pins and encoders, defining the constant parameters, starting up the brushless DC motors, implementing the main control loop, and plotting the results. The main control loop reads the position feedback of the two encoders and computes the velocity of them. Then the SDC matrices are updated, and the control gain is found by solving the SDRE. The next step is defining control law and mapping it to the servo scale. The control law is also bounded to the min/max servo limits.

6. Results

6-1. Simulations

The one-DoF design is visited briefly since the focus of the work is on the second model. The negative thrust is highlighted with the pure rotation model, Fig. 5, which needed the input signal presented in Fig. 6, generated by the exact solution to the Riccati equation (15).

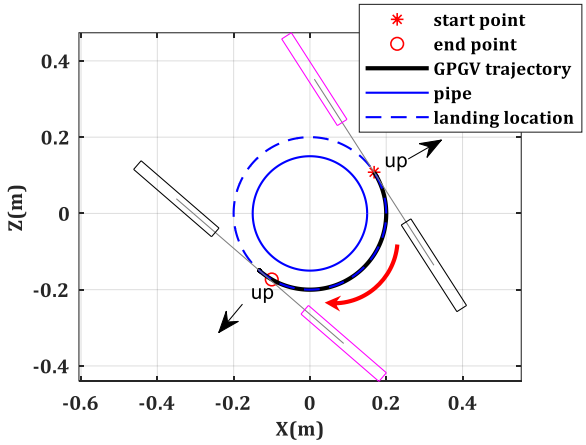

Fig. 5. A regulation under the pipe with help of the VP rotor; one-DoF system.

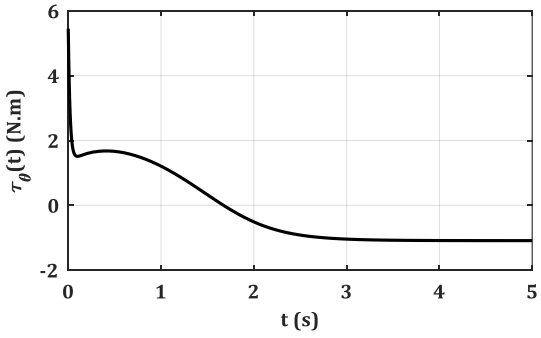

Fig. 6. Input torque of one-DoF system using the exact solution to the Riccati equation.

To show the advantages of the variable-pitch rotor quadcopters in comparison with fixed-pitch systems, the system has been implemented in simulation. A representative simulation experiment considers the two-DoF model on a pipe under a wind gust (vanishing disturbance) deviated from the top desired position, as a disturbance vector

Preprint version of the article:
S. R. Nekoo, J. A. Acosta, G. Heredia, and A. Ollero, "A benchmark mechatronics platform to assess the inspection around pipes with variable pitch quadrotor for industrial sites," Mechatronics (79): 2021, 102641, 1-9.
DOI: https://doi.org/10.1016/j.mechatronics.2021.102641

$$\mathbf{d}(t) = W_{\text{eff}}\, A_{\text{eff}} \exp(-t) \begin{bmatrix} \cos\big(\varphi_{\text{wind}} - \theta(t)\big) \\ \sin\big(\varphi_{\text{wind}} - \theta(t)\big) \end{bmatrix}, \tag{20}$$

where $W_{\text{eff}} = 10\ (\text{m}^{-1}\text{s}^{-2})$ is the weight of the wind, $A_{\text{eff}} = 0.5675\ (\text{m}^2)$ is the effective area and $\varphi_{\text{wind}} = \pi/4\ \ (\text{rad})$. The disturbance vector (20) is added to the lower part of the system (4) to represent the presence of wind gust in the simulation. The proposed SDRE controller (18) closes the control loop. The time of simulation was set to 5 seconds. The control gains were defined as $\mathbf{R} = \mathbf{I}_{2\times 2}$ and $\mathbf{Q} = \text{diag}[1,0.01,2,0.02]$. The radius of the pipe was assumed 15cm. The initial condition was set as $\pi/6$ rad rotary distance from equilibrium point and 2cm away from pipe; the desired position, without loss of generality is the equilibrium point.

In Fig. 7, the wind gust provides a force/weight ratio >1 making that the fixed-pitch one fails under its impossibility of generating a counteracting negative thrust. In Fig. 8, with the force/weight ratio <1 the fixed-pitch one can recover but, it was forced to an undesirable excursion. However, in both cases the variable-pitch one succeeded in reaching the target near the pipe, overcoming such disturbance. The capability of the VP rotor quadcopter is shown in Fig. 9 and Fig. 10, for generating negative thrust to recover better from such inconvenient disturbance while fixed-pitch was unable to generate the negative force.

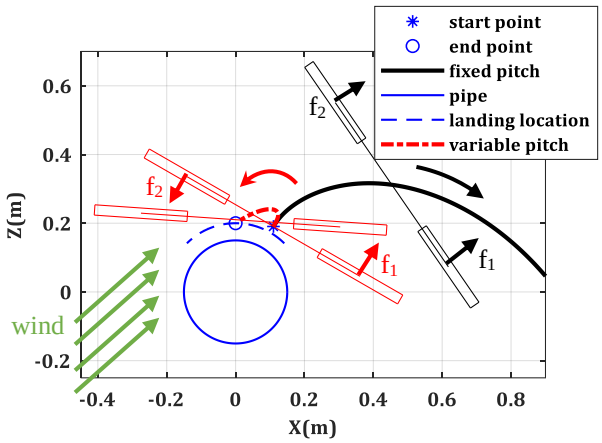

Fig. 7. The comparison between VP rotor and fixed-pitch system; force/weight ratio >1.

Preprint version of the article:
S. R. Nekoo, J. A. Acosta, G. Heredia, and A. Ollero, "A benchmark mechatronics platform to assess the inspection around pipes with variable pitch quadrotor for industrial sites," Mechatronics (79): 2021, 102641, 1-9.
DOI: https://doi.org/10.1016/j.mechatronics.2021.102641

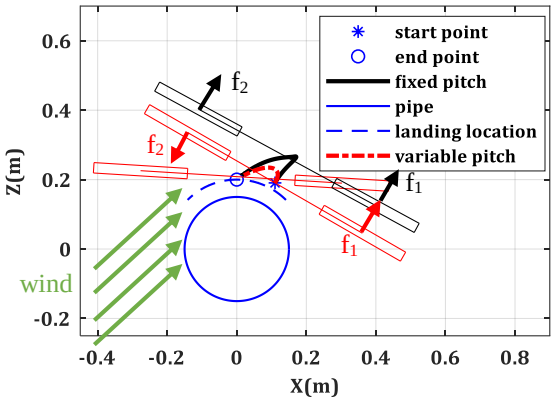

Fig. 8. The comparison between VP rotor and fixed-pitch system; force/weight ratio <1.

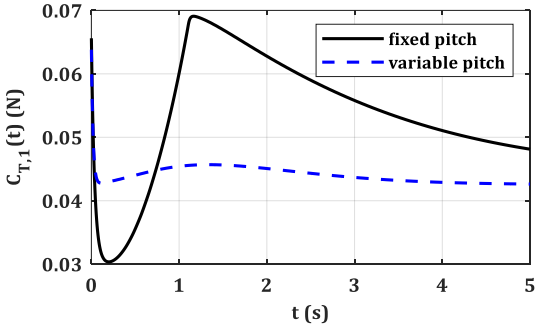

Fig. 9. Thrust coefficient of the first rotor.

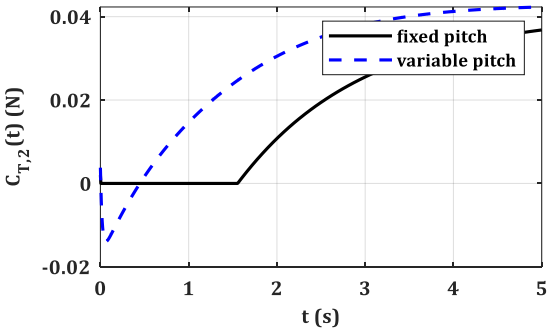

Fig. 10. Thrust coefficient of the second rotor.

6-2. Experiments

6-2-1. One-DoF experiment

An experiment has been defined to show the capability of the system to regulate in different positions in the workspace. First, the system should regulate to zero, equilibrium point, and stays there for 12s. Then regulation to $+30^{\circ}$ and -20° is required, staying 6s at each point. The details of the control task are presented in Fig. 11. The variation of θ and $\dot{\theta}$ are presented in Fig. 12 and Fig. 13 with respect. The computed torque for the regulation task is plotted in Fig. 14.

Preprint version of the article:
S. R. Nekoo, J. A. Acosta, G. Heredia, and A. Ollero, “A benchmark mechatronics platform to assess the inspection around pipes with variable pitch quadrotor for industrial sites,” Mechatronics (79): 2021, 102641, 1-9.
DOI: https://doi.org/10.1016/j.mechatronics.2021.102641

The mapping of the input torque resulted in servo commands in Fig. 15. Since the one-DoF system does not have the gravity effect and only one single input torque is available, the actuation of the servos for blade angles is similar, but in opposite directions. A sequence of images representing the experiment is shown in Fig. 16 to illustrate different regulation points in the control task.

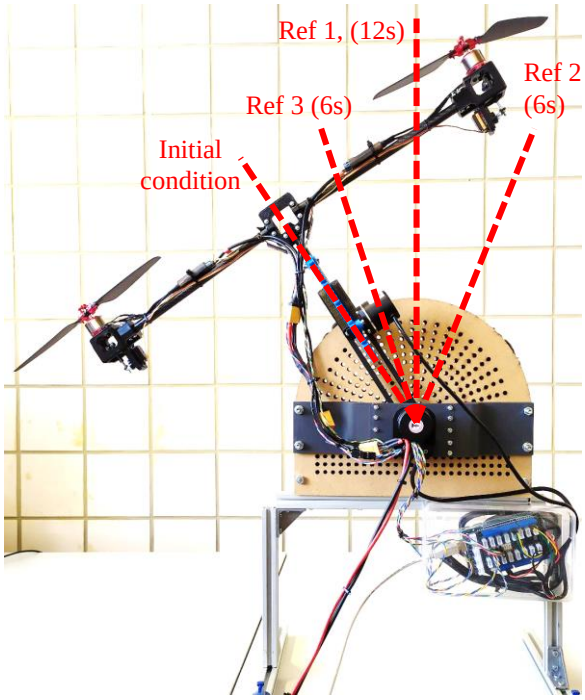

Fig. 11. Details of the regulation task in one-DoF mode.

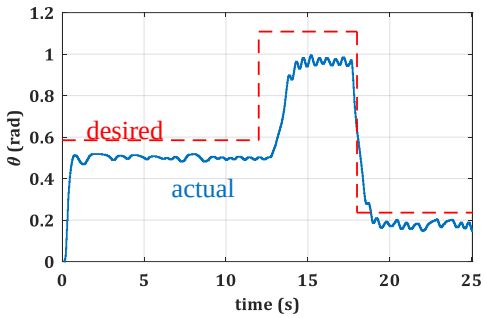

Fig. 12. Variation of θ in one-DoF experiment.

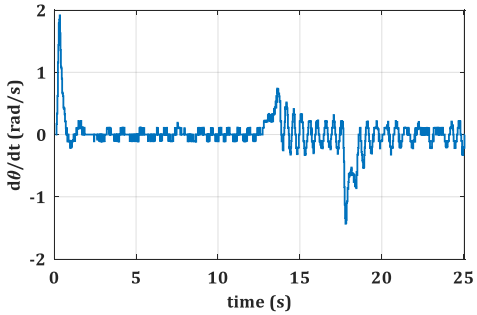

Fig. 13. Angular velocity of the system in the one-DoF experiment.

Preprint version of the article:
S. R. Nekoo, J. A. Acosta, G. Heredia, and A. Ollero, "A benchmark mechatronics platform to assess the inspection around pipes with variable pitch quadrotor for industrial sites," Mechatronics (79): 2021, 102641, 1-9.
DOI: https://doi.org/10.1016/j.mechatronics.2021.102641

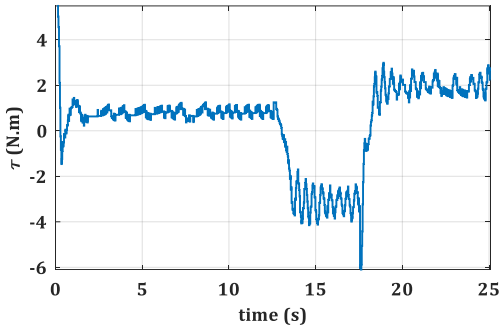

Fig. 14. Input torque to the one-DoF rotary system.

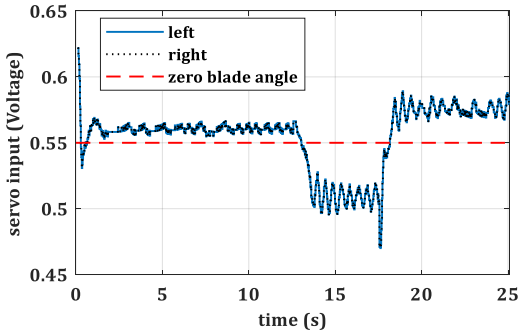

Fig. 15. Blade angles in the one-DoF experiment.

(1) (2)

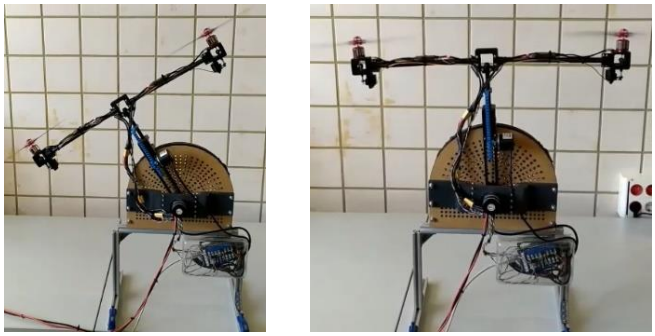

(3) (4)

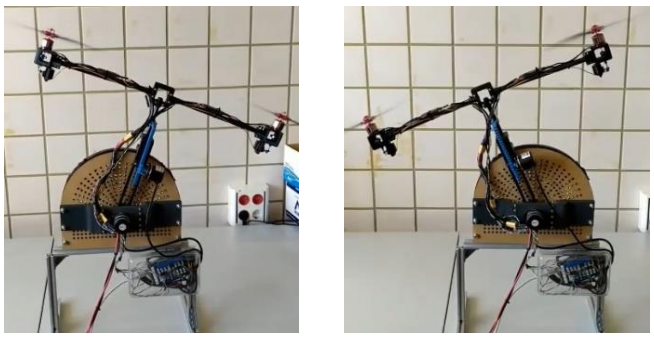

Fig. 16. A sequence of images, representing the different phases of experiments; (1) system at rest, (2) regulation to equilibrium point, (3) regulation to the first point, (4) regulation to the second point.

Preprint version of the article:
S. R. Nekoo, J. A. Acosta, G. Heredia, and A. Ollero, "A benchmark mechatronics platform to assess the inspection around pipes with variable pitch quadrotor for industrial sites," Mechatronics (79): 2021, 102641, 1-9.
DOI: https://doi.org/10.1016/j.mechatronics.2021.102641

6-2-2. Two-DoF experiment

The initial condition of the system is selected as $\theta(0) = -0.6257\text{rad}, r(0) = 0.0164\text{m}$, and the final condition was set on the equilibrium point. The initial and desired velocities are also zero for the regulation case. The control gains were chosen as $\mathbf{R} = \mathbf{I}_{2\times 2}$ and $\mathbf{Q} = \text{diag}[1.5,15,0.5,0.75]$. The PWM of the brushless DC motors is working with 68% of the power. The gap of implementation between theory and the experiment always exist and must be minimized. The left DC motor rotates clockwise (from the top view) and the right one rotates counterclockwise. The servo setup and rotation of the BLDC impose the same direction for the actuation of the servos to have a different thrust in rotors (results of the different rotational direction of rotors). One of the challenges for VP rotor systems is the asymmetrical blade mechanism. This means the blade motion range and the distance are different on each side. The generated control input (18) is transformed into servo commands by

$$\begin{aligned} U_{\text{serv,L}} &= U_{\text{serv,0}} + \frac{k_s}{l}u_2(t) - k_s u_1(t) - U_{\text{c,L}}, \\ U_{\text{serv,R}} &= U_{\text{serv,0}} + \frac{k_s}{l}u_2(t) + k_s u_1(t) + U_{\text{c,R}}, \end{aligned} \tag{21}$$

where $U_{\text{serv,0}}$ locates the servo at zero blade angle, $k_s = 2.91 \times 10^{-3}$ is a constant for adjusting the input into the servo scale, l has the same definition and value in Table 1, $U_{\text{c,L}} = 0.02$ and $U_{\text{c,R}} = 0.01$ compensate the weight. The values of $U_{\text{c,L}}$ and $U_{\text{c,R}}$ should not be high to avoid interference in the regulation signal. They are not symmetric since the VP blade mechanism is not symmetric. The objectives of the experiment were two points, implementation of the SDRE as a nonlinear closed-loop optimal control online and achieving maneuver in a framework similar to rotation around a pipe. Both of them were achieved successfully. The input $u_2(t)$ is related to rotary motion and $u_1(t)$ to radial one. If we compare (21) with (19), one could see that they are compatible and the difference in the signs is compensated with the opposite rotational motion of the BLDC and servo actuation. The experiment was carried out with 700 samples, in 25.1s, Fig. 17. The errors of rotary motion and radial one are depicted in Fig. 18 and Fig. 19 with respect. The servo inputs are presented in Fig. 20; they reached steady-state values to hold the system on the desired radial position. The directions are opposite though thrust is correctly imposed. Finally, the input force and torque are illustrated in Fig. 21 and Fig. 22.

The prototype is heavier than it was expected due to the measurement system and using cables. That made it hard for the system to perform flight outward though from any initial

Preprint version of the article:
S. R. Nekoo, J. A. Acosta, G. Heredia, and A. Ollero, "A benchmark mechatronics platform to assess the inspection around pipes with variable pitch quadrotor for industrial sites," Mechatronics (79): 2021, 102641, 1-9.
DOI: https://doi.org/10.1016/j.mechatronics.2021.102641

position, it could regulate to the desired position $r_{\text{des}} < r_{\text{initial}}$. This drawback will be amended by using an onboard measurement system and stronger motors in the next version of the setup.

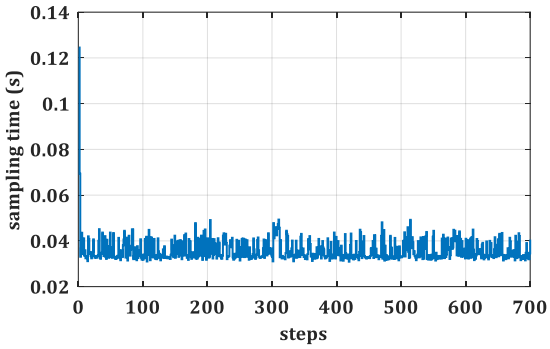

Fig. 17. Time-varying sampling time.

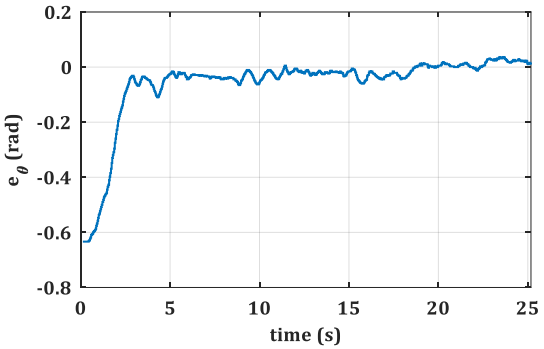

Fig. 18. The rotational error in the experiment.

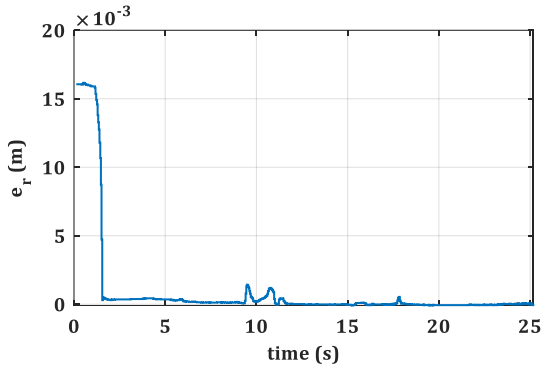

Fig. 19. Radial error in the experiment.

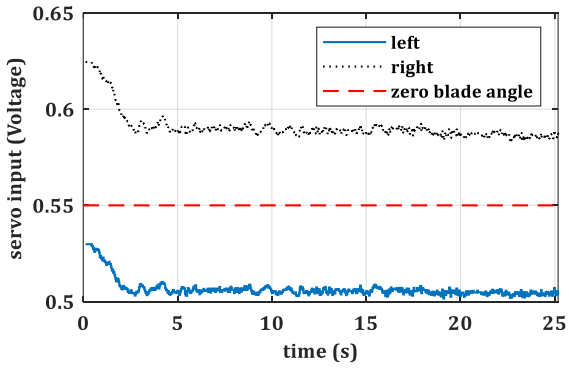

Fig. 20. Servo input is applied to the rotors in the experimental platform.

Preprint version of the article:
S. R. Nekoo, J. A. Acosta, G. Heredia, and A. Ollero, "A benchmark mechatronics platform to assess the inspection around pipes with variable pitch quadrotor for industrial sites," Mechatronics (79): 2021, 102641, 1-9.
DOI: https://doi.org/10.1016/j.mechatronics.2021.102641

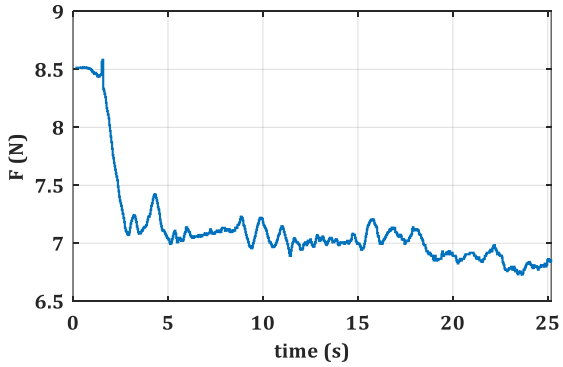

Fig. 21. Computed input force, thrust.

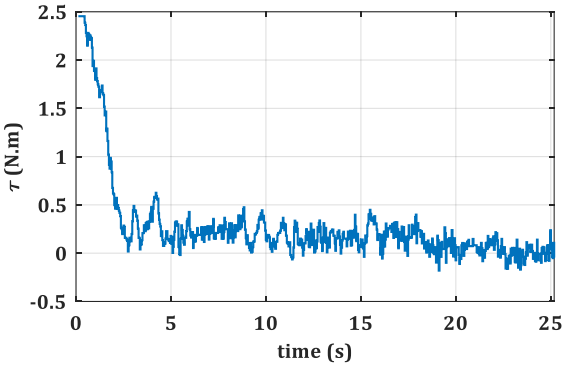

Fig. 22. Computed input torque.

7. Conclusions

This work presented a novel experimental platform for investigating the VP rotor quadcopters for inspection while rotating around a pipe. Two models were proposed for simulating the maneuver, one- and two-degree-of-freedom. Both of them could be tested with the testbed. The state-dependent Riccati equation controller was employed for regulation problems. The SDRE is a nonlinear optimal controller and hardly tested online without simplification. In this work, the SDRE was implemented online preserving the nonlinear structure. In each time-step, the Riccati equation was solved in the control loop and the average sampling time was 0.04s. This research was the primary design of a VP system for the inspection of pipes. The weight of the system must be reduced for the next prototype with onboard communication systems and measurement to close the design to reality for better tests.

Acknowledgements

This work is supported by the HYFLIERS project (HYbrid FLying-rolling with-snakE-aRm robot for contact inspection) funded by the European Commission H2020 Programme under

grant agreement ID: 779411 (https://cordis.europa.eu/project/rcn/213049) and the ARTIC (RTI2018-102224-B-I00) project, funded by the Spanish Agencia Estatal de Investigación.

References

[1] P. M. Kornatowski, S. Mintchev, and D. S. Floreano, "An origami-inspired cargo drone," in *2017 IEEE/RSJ International Conference on Intelligent Robots and Systems (IROS)*, Vancouver, BC, Canada, 2017, pp. 6855-6862.
[2] M. Á. Trujillo, J. R. Martínez-de Dios, C. Martín, A. Viguria, and A. Ollero, "Novel aerial manipulator for accurate and robust industrial NDT contact inspection: A new tool for the oil and gas inspection industry," *Sensors*, vol. 19, p. 1305, 2019.
[3] Á. Montes-Romero, A. Torres-González, J. Capitán, M. Montagnuolo, S. Metta, F. Negro, *et al.*, "Director Tools for Autonomous Media Production with a Team of Drones," *Applied Sciences*, vol. 10, p. 1494, 2020.
[4] S. V. Sibanyoni, D. T. Ramotsoela, B. J. Silva, and G. P. Hancke, "A 2-D acoustic source localization system for drones in search and rescue missions," *IEEE Sensors Journal*, vol. 19, pp. 332-341, 2018.
[5] G. Aiello, F. Hopps, D. Santisi, and M. Venticinque, "The Employment of Unmanned Aerial Vehicles for Analyzing and Mitigating Disaster Risks in Industrial Sites," *IEEE Transactions on Engineering Management*, 2020.
[6] H. Guo, Q. Cui, J. Wang, X. Fang, W. Yang, and Z. Li, "Detecting and Positioning of Wind Turbine Blade Tips for UAV-Based Automatic Inspection," in *IGARSS 2019-2019 IEEE International Geoscience and Remote Sensing Symposium*, Yokohama, Japan, Japan, 2019, pp. 1374-1377.
[7] P. J. Sanchez-Cuevas, P. Ramon-Soria, B. Arrue, A. Ollero, and G. Heredia, "Robotic system for inspection by contact of bridge beams using UAVs," *Sensors*, vol. 19, p. 305, 2019.
[8] T. Mao, K. Huang, X. Zeng, L. Ren, C. Wang, S. Li, *et al.*, "Development of Power Transmission Line Defects Diagnosis System for UAV Inspection based on Binocular Depth Imaging Technology," in *2019 2nd International Conference on Electrical Materials and Power Equipment (ICEMPE)*, Guangzhou, China, China, 2019, pp. 478-481.
[9] S. Marathe, "Leveraging drone based imaging technology for pipeline and RoU monitoring survey," in *SPE Symposium: Asia Pacific Health, Safety, Security, Environment and Social Responsibility*, Kuala Lumpur, Malaysia, 2019.
[10] M. Perez, A. Suarez, G. Heredia, and A. Ollero, "Positioning System for Pipe Inspection with Aerial Robots Using Time of Flight Sensors," in *Iberian Robotics conference*, 2019, pp. 16-27.
[11] https://www.oulu.fi/hyfliers/.
[12] A. Lopez-Lora, P. J. Sanchez-Cuevas, A. Suarez, A. Garofano, A. Ollero, and G. Heredia, "MHYRO: Modular HYbrid RObot for contact inspection and maintenance in oil&gas plants," in *IEEE/RSJ International Conference on Intelligent Robots and Systems (IROS)*, Nevada, Las Vegas, 2020.
[13] S. Zhao, F. Ruggiero, G. A. Fontanelli, V. Lippiello, Z. Zhu, and B. Siciliano, "Nonlinear Model Predictive Control for the Stabilization of a Wheeled Unmanned Aerial Vehicle on a Pipe," *IEEE Robotics and Automation Letters*, vol. 4, pp. 4314-4321, 2019.
[14] T. H. Bane, "Recent advances in aviation," SAE Technical Paper 0148-7191, 1920.
[15] C. K. Neilsen Jr, "A summary of controllable pitch propeller systems employed by the US navy," *Naval Engineers Journal*, vol. 86, pp. 81-90, 1974.
[16] R. V. Petrescu, R. Aversa, B. Akash, J. Corchado, F. Berto, A. Apicella, *et al.*, "About helicopters," *Journal of Aircraft and Spacecraft Technology*, vol. 1, pp. 204-223, 2017.
[17] D. Langkamp and W. J. Crowther, "The role of collective pitch in multi rotor UAV aerodynamics," *European Rotorcraft Forum*, 2010.
[18] M. Cutler, N.-K. Ure, B. Michini, and J. How, "Comparison of fixed and variable pitch actuators for agile quadrotors," in *AIAA Guidance, Navigation, and Control Conference*, 2011, pp. 6406-6423.
[19] M. Cutler and J. How, "Actuator constrained trajectory generation and control for variable-pitch quadrotors," in *AIAA Guidance, Navigation, and Control Conference*, 2012, p. 4777.
[20] M. E. McKay, R. Niemiec, and F. Gandhi, "Performance comparison of quadcopters with variable-RPM and variable-pitch rotors," *Journal of the American Helicopter Society*, vol. 64, pp. 1-14, 2019.
[21] M. Bhargavapuri, S. R. Sahoo, and M. Kothari, "Robust nonlinear control of a variable-pitch quadrotor with the flip maneuver," *Control Engineering Practice*, vol. 87, pp. 26-42, 2019.
[22] S. R. Nekoo, J. Á. Acosta, A. E. Gomez-Tamm, and A. Ollero, "Optimized thrust allocation of variable-pitch propellers quadrotor control: A comparative study on flip maneuver," in *2019 Workshop on Research,*

Education and Development of Unmanned Aerial Systems (RED UAS), Cranfield, United Kingdom, United Kingdom, 2019, pp. 86-95.

[23] A. Fradkov, B. Andrievsky, and K. Boykov, "Control of the coupled double pendulums system," *Mechatronics*, vol. 15, pp. 1289-1303, 2005.

[24] L. Tang, X. Tang, X. Jiang, and C. Gosselin, "Dynamic trajectory planning study of planar two-dof redundantly actuated cable-suspended parallel robots," *Mechatronics*, vol. 30, pp. 187-197, 2015.

[25] A. L. Fradkov, B. Andrievsky, and K. B. Boykov, "Multipendulum mechatronic setup: Design and experiments," *Mechatronics*, vol. 22, pp. 76-82, 2012.

[26] J. R. Cloutier, "State-dependent Riccati equation techniques: An overview," in *Proceedings of the 1997 American Control Conference* Albuquerque, New Mexico, 1997, pp. 932-936.

[27] A. Jagat and A. J. Sinclair, "Nonlinear control for spacecraft pursuit-evasion game using state-dependent Riccati equation method," *IEEE Transactions on Aerospace and Electronic Systems*, vol. 53, pp. 3032-3042, 2017.

[28] A. Fenili, "The rigid-flexible robotic manipulator: Nonlinear control and state estimation considering a different mathematical model for estimation," *Shock and Vibration*, vol. 20, pp. 1049-1063, 2013.

[29] J. Lee, Y. Lee, Y. Kim, G. Moon, and B.-E. Jun, "Design of an adaptive missile autopilot considering the boost phase using the SDRE method and neural networks," *Journal of the Franklin Institute*, vol. 355, pp. 9085-9107, 2016.

[30] T. D. Do, S. Kwak, H. H. Choi, and J.-W. Jung, "Suboptimal control scheme design for interior permanent-magnet synchronous motors: An SDRE-based approach," *IEEE Transactions on Power Electronics*, vol. 29, pp. 3020-3031, 2014.

[31] A. M. Tusset, A. M. Bueno, J. P. M. dos Santos, M. Tsuchida, and J. M. Balthazar, "A non-ideally excited pendulum controlled by SDRE technique," *Journal of the Brazilian Society of Mechanical Sciences and Engineering*, vol. 38, pp. 2459-2472, 2016.

[32] M. A. Ribeiro, J. M. Balthazar, W. B. Lenz, R. T. Rocha, and A. M. Tusset, "Numerical exploratory analysis of dynamics and control of an atomic force microscopy in tapping mode with fractional order," *Shock and Vibration*, vol. 2020, 2020.

[33] H. Voos, "Nonlinear state-dependent Riccati equation control of a quadrotor UAV," in *IEEE Computer Aided Control System Design, IEEE International Conference on Control Applications, IEEE International Symposium on Intelligent Control*, Munich, Germany, 2006, pp. 2547-2552.

[34] S. Jing-Liang, L. Chun-Sheng, L. Ke, and S. Hao-Ming, "Optimal robust control for attitude of quad-rotor aircraft based on SDRE," in *34th Chinese Control Conference*, Hangzhou, China, 2015, pp. 2333-2337.

[35] B. Geranmehr, E. Khanmirza, and S. Kazemi, "Trajectory control of aggressive maneuver by agile autonomous helicopter," *Proceedings of the Institution of Mechanical Engineers, Part G: Journal of Aerospace Engineering*, p. 0954410018755807, 2018.

[36] M. Bhargavapuri, S. R. Sahoo, and M. Kothari, "Robust attitude tracking in the presence of parameter uncertainty for a variable-pitch quadrotor," in *American Control Conference*, Wisconsin Center, Milwaukee, USA, 2018, pp. 3454-3459.

[37] T. Cimen, "Survey of state-dependent Riccati equation in nonlinear optimal feedback control synthesis," *Journal of Guidance, Control, and Dynamics*, vol. 35, pp. 1025-1047, 2012.

[38] S. R. Nekoo, "Tutorial and Review on the State-dependent Riccati Equation," *Journal of Applied Nonlinear Dynamics*, vol. 8, pp. 109-166, 2019.

[39] M. H. Korayem and S. R. Nekoo, "Finite-time state-dependent Riccati equation for time-varying nonaffine systems: Rigid and flexible joint manipulator control," *ISA Transactions*, vol. 54, pp. 125-144, 2015.

[40] S. R. Nekoo, "Digital implementation of a continuous-time nonlinear optimal controller: An experimental study with real-time computations," *ISA transactions*, vol. 101, pp. 346-357, 2020.